Eur. Phys. J. D **46**, 111–127 (2008)
DOI: 10.1140/epjd/e2007-00284-4

THE EUROPEAN PHYSICAL JOURNAL D

Multiparametric dependence of hydrogen Stark profiles asymmetry

A.V. Demura[1,a], G.V. Demchenko[1], and D. Nikolić[2,b]

[1] IVEPT, RRC "Kurchatov institute", Kurchatov Square 1, Moscow 123182, Russia
[2] Department of Physics, Western Michigan University, Kalamazoo MI-49008, USA

Received 5 May 2007 / Received in final form 10 September 2007
Published online 5 October 2007 – © EDP Sciences, Società Italiana di Fisica, Springer-Verlag 2007

Abstract. The Standard Theory for hydrogen spectral lines asymmetry in dense plasmas is developed on the basis of rigorous and consistent approach with respect to simultaneous and complete account of the quadrupole interaction and the quadratic Stark effect. The complex multiparametric scaling and similarity dependence of the conventional asymmetry parameter for each separate Stark component and the H_β line contour as a whole is revealed and studied in detail under the influence of: ionic microfield inhomogeneity and quadratic Stark effect in ionic microfield, electronic collision shifts and impact widths, "trivial" asymmetry sources, the Boltzmann factor and the dipole intensity scaling factor of frequency to the fourth power for the case of emission line. The comparison with the precision experiment on stabilized arc data for H_β line, important for diagnostics, is performed and analyzed from the line center up to the far line wings.

PACS. 32.70.Jz Line shapes, widths, and shifts – 32.60.+i Zeeman and Stark effects – 52.20.Fs Electron collisions – 52.20.Hv Atomic, molecular, ion, and heavy-particle collisions

1 Introduction

The phenomena of asymmetry of hydrogen Stark profiles in plasmas is attracting attention since the first observations [1]. Many experimental [2–16] and theoretical [14–46] studies follow, identifying various sources of asymmetry and explaining some of their characteristics [14–46]. But nevertheless the satisfactory exact, ample and reconcilable treatment of experimental data was not achieved until recently [14,15]. In particular, the results of the recent series of papers [32,36,39], operating with the corrections to frequencies due to the quadratic Stark effect (QSE) and the electron collision shifts, introduced by Griem [47], demonstrated the good coincidence with experiment. However, under the attempts to reproduce these results it was ascertained that omitted in [32,36,39] QSE corrections to intensities strongly suppress the QSE asymmetry and could not allow for coincidence with experiment on which authors of [32,36,39] pretended. It was declared in those works that the multiplicative ω^4 factor (that scales the dipole radiation intensity and conventionally discarded under the contour representation in order to achieve the normalization to unity in the infinite limits of integration over the frequency detuning from the line center), and the Boltzmann factor with the current frequency values [19,48–50] were included in calculations. But it is worthy to mention that the question of taking the latter factors into account is still under discussion as from the point of view of requests to self-consistency of the theoretical approach, as from the point of view of implementation of the adequate experimental methodics to the contour separation on the background of continuum [14,15]. Indeed, the Boltzmann factor with the current frequency of radiation appears under writings of the Kirchhoff's law for the continuum spectra [48–50], and seems to be valid for the case of the individual spectral lines as well. Nevertheless this way of representation for the discrete spectrum is not conventional and usually relates the Boltzmann factor to the unperturbed frequency of radiative transition [48]. The testing of the influence of latter factors on asymmetry of H_β line has been performed recently in [14,15], where it was shown that their direct introduction in the asymmetry description leads to an increased deviation from the experiment both quantitatively and qualitatively, which contradicts to statements found in [32,36]. At the same time analysis of [14,15] revealed that the implementation of perturbation theory in the contour on quadrupole interaction without expansion over the QSE correction to frequency (due to divergence arising under the integration over ion microfield strengths) is not fully consistent [44]. That is why the urgent request have arisen to perform the detailed study of asymmetry on the basis of

[a] e-mail: Alexander.Demura@hepti.kiae.ru
[b] e-mail: dragan.nikolic@wmich.edu

non-perturbative methods. The only presently known non-perturbative analytic approach to the description of multiplicative statistical problem (see [26,37]) is based on the consideration of Hamiltonian of interaction averaged over the components of microfield non-uniformity tensor, the electric ion microfield strength vector being fixed. This is more adequate for the case of taking into account QSE (compare [14,15,23]). One of the forcible arguments for the implementation of this approximation is that in the binary limit it is fulfilled exactly [22]. Thus the present work is devoted to the detailed theoretical study of asymmetry of hydrogen spectral lines in dense plasmas that is logically and conceptually connected with the previously published works on this subject [14,15,23,30]. The significant moment in this study is the demonstration of strong influence of "trivial asymmetry" (emerging during conversion from the frequency scale to the wavelength scale) on the qualitative and quantitative behavior of the asymmetry parameter. At the same time the influence of transition from the impact broadening regime to the quasistatic one in the far line wings [48,49,33] and the role of ion dynamics [46,51,52] are discussed. Thus as the asymmetry of hydrogen Stark profiles in plasmas is shown to be the extremely sensitive function of broadening mechanisms [44] its study becomes fundamentally significant.

The article is organized as follows: after the introduction in Section 1, main ideas of approximate description of joint statistics of the ion microfield and its spatial derivatives are given in Section 2; Section 3 introduces general expressions for the asymmetrical Stark profiles, followed by Section 4 containing main formulas for the electron impact widths together with corrections for shifts and intensities for Stark components due to the interaction with ionic microfield and its gradients; Section 5 contains detailed analysis of main effects that induce the asymmetry of Stark profiles and comparison with experimental results; Section 6 is devoted to discussion of the status of the present and other approaches; finally, obtained results are formulated in Section 7 followed by acknowledgments and references.

2 First moments approximation for joint distribution functions of microfield and its spatial derivatives

For consideration of the problem of the profile asymmetry it is insufficient to know only the microfield distribution, as the Hamiltonian of hydrogen atom interaction with plasma particles contains besides the dipole interaction term (expressed through the scalar product of the resulting summary microfields due to ions and electrons and the vector of the atomic dipole operator), also the following terms of the interaction potential expansion over parameter $\varepsilon = n^2/R_0 \ll 1$, where R_0 — is the mean interparticle distance in atomic units [20,23]. The first such term, quadratic over components of coordinates of atomic electrons, is the quadrupole interaction, determined by convolution of tensor $\partial F_i/\partial x_k$ — that is composed from spatial derivatives of various components of the ion electric microfield strength vector $\boldsymbol{F}$, and operator of atomic quadrupole moment Q_{ik} with appropriate numerical coefficients 1/6 and negative sign (see [23]).

This means that — within quasistatic approximation — the description of broadening requires the knowledge of spatial distribution functions of various configurations of perturbing particles. As a consequence, the joint distribution functions $W\left(\boldsymbol{F};\{\partial F_i/\partial x_k\}\right)$ of the electric microfield vector $\boldsymbol{F}$ and all independent components of the tensor, composed from its spatial derivatives $\partial F_i/\partial x_k$ [23], should be introduced [23].

So complex multi-parametric distribution functions are not calculated yet up to now and that is why the approximate description is used with the help of the first moments of this complete joint distribution function over the various components of microfield tensor of non-uniformity $\{\partial F_i/\partial x_k\}$ [23,24,26].

The tensor of moments of this function is symmetrical and in the case of Coulombic field has zero trace. It was shown in [23,24] that the solution of quantum mechanical problem of calculating the corrections in the first order of perturbation theory for many-body quadrupole interaction is expressed in the reference frame with OZ axis along the microfield vector $\boldsymbol{F}$. Such solutions incorporate the product of the component Q_{zz} of the operator of atomic quadrupole moment and the universal function $B\left(\beta\right)$ of the reduced microfield value $\beta = F/F_0$ (F_0 is the normal Holtsmark field strength), which determines the behavior of first moments of microfield non-uniformity tensor versus β for chosen construction of joint distribution functions (see [52]). For Holtsmark distribution $W_H(\beta)$ [48,49,52,53] this function could be represented in the form [23,52]

$$B\left(\beta\right) = \frac{3\int\limits_0^\beta W_H\left(\beta'\right)d\beta'}{W_H\left(\beta\right)} - 1. \tag{1}$$

The graph of $B\left(\beta\right)$ and its analog $2\beta^{3/2}$, corresponding to the nearest neighbor distribution $W_{NN}(\beta)$ [53] are represented in Figure 1, while the instructive comparison of $W_H(\beta)$ and $W_{NN}(\beta)$ distributions is given in Figure 2.

This result, in the first order of perturbation theory over parameter ε, allows us to find expressions for the intensity and the electron impact width due to the many-body quadrupole interaction [23]. As it was already pointed out in the introduction, here we made an attempt to include the influence of quadratic Stark effect [54,55] more consistently than what has been done earlier in [26,32,36,39], accounting for corrections to the wave functions due to the quadratic Stark effect (QSE) and the corresponding deviations in the intensity of Stark components [55]. However, it is necessary to note that at the same time the quadratic corrections over parameter ε^2 to the wave functions are accounted for only partially (in particular, only those provided by the QSE corrections) [20,23] while corrections to the frequency in the first order of octupole interaction, proportional to ε^4 [20],

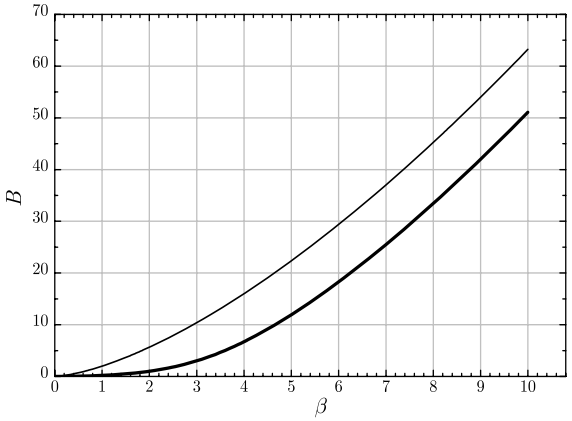

Fig. 1. Comparison of universal functions describing the first moment of the microfield nonuniformity tensor in the case of the Holtsmark distribution $B(\beta)$ (thick line) and in the case of the nearest neighbor distribution $2\beta^{3/2}$ (thin line).

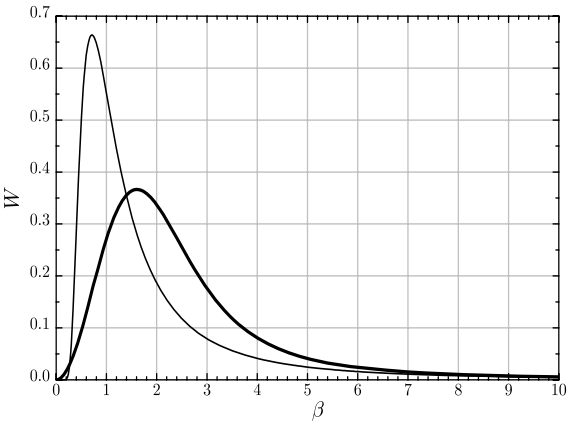

Fig. 2. Comparison of the Holtsmark (thick line) and nearest neighbor distributions (thin line).

such as the QSE shift, are not taken into account at all. Indeed, in this problem corrections to frequency in the first order of various interactions are arranged in series over powers of parameter ε in the following way: the linear Stark effect $\sim\varepsilon^2$, the quadrupole interaction $\sim\varepsilon^3$, the octupole interaction and QSE $\sim\varepsilon^4$ etc. [20]. The corrections to the wave functions from the first order of the quadrupole interaction are proportional to ε, and the corrections to the wave functions in the next order, proportional to ε^2, are produced by contributions from the first order of QSE and the octupole interaction and from the second order of the quadrupole interaction (QI) [20]. Thus beyond the sight there are corrections to the frequency and wave functions from the octupole interaction in the first order and the corrections to the wave functions from the quadrupole interaction in the second order (see [20]). This is, of course, violation of the consistent construction of asymptotic perturbation series [54]. But on the other side in the frames of many-body approach the realization of consistent scheme is not possible since corresponding moments of the octupole and the quadrupole interaction are not known yet [23,52]. Further analysis of a part of matrix elements of corresponding expressions revealed their symmetry with respect to the difference $(n_1 - n_2)$ (see [20]). This means that these terms will not contribute to asymmetry, but only to the line profile. Thus the pointed out peculiarities justify the present settings in spite of incomplete account of all corrections in the "second order" over parameter ε — in the fourth power to the frequency and in the second power to wave functions.

In the first attempt to realize this, computation was carried out by Demura and Nikolić [14,15,42]. In the frames of the perturbation approach Nikolić created general code in *Mathematica* programming package, that was used for modeling of experimental results found in [14,15]. However, our previous work [14,15,42] used the perturbation theory in the contour over the quadrupole interaction, which is not completely correct when retaining the QSE in the resolvent.

In order to avoid the perturbation expansion in the line contour we used the method of statistically averaged Hamiltonian over the non-uniformity tensor components [26]. Present work traces each Stark component and investigates the character of the formation of the profile asymmetry under the influence of various sources. As a result, additional dependences were revealed due to the inclusion of QSE, previously unnoticed in [14,15,26,32,36,39].

For the purpose of theoretical calculations Demchenko created the C++ code, which allows us to efficiently perform necessary computations.

3 Standardized theory for asymmetrical Stark profiles in plasmas

As it was already pointed out in the introduction it is assumed in the present work as in [14,15,20–24,30,42,44] that the electron broadening in plasmas could be described in the no quenching and impact approximations, whilst the broadening by plasma ions in the quasistatic approximation [48,49]. For study of the Stark profiles behavior it is useful to implement the parabolic basis of wave functions for hydrogen-like radiators [54]. Then formally for the averaged quadrupole ion-radiator interaction under the fixed reduced value of ion electric microfield β the normalized Stark profile of spectral line $I_{n,n'}(\beta;\Delta\omega)$, corresponding to the transition $n \to n'$ between the upper and lower states with principal quantum numbers n and n', could be represented as the sum of the isolated profiles of Stark components (sub-lines) $I_k(\beta;\Delta\omega)$ in the diagonal approximation for the electron impact broadening operator [23,30]

$$I_{n,n'}(\beta;\Delta\omega)d\omega = \sum_k I_k(\beta;\Delta\omega)d\omega = \sum_k \frac{\Pi_k(\beta)}{\gamma_k(\beta)} L\left(\frac{\Delta\omega - d_k^{(e)} - s_k(\beta)}{\gamma_k(\beta)}\right) d\omega \quad (2)$$

$$\Pi_k(\beta) = \Pi_k^{(0)}\mathcal{I}_k(\beta), \quad \Pi_k^{(0)} = \left(\frac{I_k}{\sum_k I_k}\right). \quad (3)$$

Here index k designates the Stark component corresponding to the transition from the upper state $\{n_1, n_2, m\} \in n$ to the lower state $\{n_1', n_2', m'\} \in n'$, $\Delta\omega = (\omega - \omega_0)$ is the detuning from the line center, defined by the unperturbed radiation frequency ω_0, of the current cyclic radiation frequency ω; $\gamma_k(\beta)$ is the electron impact width of the Stark component [23,24,56]; $d_k^{(e)}$ is the electron collision shift of the individual Stark component that practically does not depend on the ion microfield [32,57,58]; $s_k(\beta)$ is the generalized ion shift of this Stark component [14,15,26,32]; $L(\Delta)$ designates the resolvent operator matrix element in the line space [59] normalized to unity under integration over the reduced frequency detuning $\Delta = (\Delta\omega - d_k^{(e)} - s_k(\beta))/\gamma_k(\beta)$; I_k is the unperturbed intensity of Stark component; $\mathcal{I}_k(\beta)$ is the generalized relative intensity of the Stark component that differs from unity due to perturbations. Effectively $L(\Delta)$ could be reduced to the Lorentzian normalized to unity under integration over Δ. In general the generalized Stark shift being the function of the reduced ion microfield value β is assumed to be compiled from the linear Stark effect shift [54], the shift due to constrained quadrupole interaction [23], the quadratic Stark effect shift [54] and the electronic collision shift [32]. And at last according to the settings of the Standard Theory of Stark broadening [48,49] the final line profile is obtained after integration of equation (1) over the reduced microfield values with the microfield distribution $W(\beta)$ as the normalized to unity weight function [52,53]:

$$I_{n,n'}(\Delta\omega)d\omega = \int_0^\infty d\beta W(\beta) I_{n,n'}(\beta;\Delta\omega)d\omega,$$
$$\int_0^\infty d\beta W(\beta) = 1. \tag{4}$$

4 Intensities, shifts and electron impact widths

After corresponding lengthy analytical computations in the considered settings using the first constrained moments approximation at fixed value of the reduced ion microfield for the description of quadrupole approximation [23,24] all quantities, entering the expression (2)–(4) for the profile of the Stark component could be expressed as functions of the reduced ion microfield β in the form (compare with [23,24,30,33,37]):

$$\mathcal{I}_k(\beta) = 1 + \delta_k \frac{B(\beta)}{\beta} + \delta_k^{qs}\beta, \tag{5}$$

$$\frac{s_k(\beta)}{s_k^d\beta} = 1 + q_k \frac{B(\beta)}{\beta} + \frac{s_k^{qs}}{s_k^d}\beta, \tag{6}$$

$$\frac{\gamma_k(\beta)}{\gamma_k^{(0)}} = 1 + P_k \frac{B(\beta)}{\beta}. \tag{7}$$

Thus $\Pi_k^{(0)}$ designates the relative unperturbed intensity of the Stark component; $s_k^d\beta$ is the frequency shift due to the linear Stark effect [54,57]; $\gamma_k^{(0)}$ is the electron impact width of the Stark component for the unperturbed zero order parabolic wave functions, that does not depend on β for the moment [23,24,56]; δ_k, δ_k^{qs} are corrections to intensity of the Stark component due to the constrained quadrupole interaction and QSE respectively; $s_k^{qs}\beta^2$ is QSE frequency shift; q_k and P_k are corrections to frequency and the electron impact width respectively due to the constrained quadrupole interaction [23].

Now the quantities introduced for the Stark component with label k in the above equations (18)–(20) could be further detailed. The constants defining the generalized shift are expressed as (compare with [20,23,30,33]):

$$s_k^d = \frac{3}{2}\Lambda a_0^2 N_e^{2/3}\Delta_k^d\omega_a, \quad q_k = \frac{2\pi}{3\Lambda}a_0 N_e^{1/3}\frac{\Delta_k^q}{\Delta_k^d}\omega_a,$$
$$s_k^{qs} = \Lambda^2 a_0^4 N_e^{4/3}\Delta_k^{qs}\omega_a, \tag{8}$$

where a_0 is the Bohr radius, ω_a is the atomic unit of frequency, N_e is the plasma electrons density with charge equal to unity, $\Lambda = 2\pi(4/15)^{2/3}$ is the constant coming from the definition of the normal Holtsmark field strength $F_0 = \Lambda e N_e^{2/3}$ [52,53]. Remind that Δ_k^d defines the relative linear Stark effect shift of the Stark level $n_1 n_2 m$ with respect to the Stark level $n_1' n_2' m'$ [23,30,33,37]

$$\Delta_k^d = n(n_1 - n_2) - n'(n_1' - n_2'), \tag{9}$$

while Δ_k^q describes the same for the quadrupole interaction [20,23,30,33,37]

$$\Delta_k^q = \frac{1}{3}\left[n^4 - n^2 - 6n^2(n_1 - n_2)^2\right] \tag{10}$$
$$- \frac{1}{3}\left[n'^4 - n'^2 - 6n'^2(n_1' - n_2')^2\right], \tag{11}$$

and Δ_k^{qs} is defined in accordance with the well-known result for QSE shift [54,55]

$$\Delta_k^{qs} = -\frac{n^4}{16}\left[17n^2 - 3(n_1 - n_2)^2 - 9m^2 + 19\right] \tag{12}$$
$$+ \frac{n'^4}{16}\left[17n'^2 - 3(n_1' - n_2')^2 - 9m'^2 + 19\right]. \tag{13}$$

The dimensionless constants defining the generalized intensity could be expressed in the form

$$\delta_k = \frac{2\pi}{3\Lambda}a_0 N_e^{1/3}\varepsilon_k^q, \quad P_k = \frac{2\pi}{3\Lambda}a_0 N_e^{1/3}\varepsilon_k^{q\gamma}$$
$$\delta_k^{qs} = \Lambda a_0^2 N_e^{2/3}\varepsilon_k^{qs}. \tag{14}$$

It is worthy to note that in (8), (14) the quantities are arranged according to the hierarchy of the contributions to the shift from various sources over the powers of the parameter $a_0 N_e^{1/3} \ll 1$, that is less than unity for the plasma densities below atomic unit. The constants defining the corrections to intensity ε_k^q and to electron impact widths $\varepsilon_k^{q\gamma}$ induced by the constrained quadrupole interaction are constructed with the help of the first order perturbation

theory to the wave functions and could be written in the form [23,24,33]

$$\varepsilon_k^q = \frac{2e^2a_0^2}{|\langle n_1n_2m|\,\boldsymbol{d}\,|n_1'n_2'm'\rangle|^2}\left(\phi^q_{n_1n_2m}+\phi^q_{n_1'n_2'm'}\right),$$
$$\varepsilon_k^{q\gamma} = \frac{2}{M_k^\gamma}\left(\phi^\gamma_{n_1n_2m}+\phi^\gamma_{n_1'n_2'm'}\right). \quad (15)$$

The corrections to intensity and electron impact widths $\phi_k^{q,\gamma}$ are expressed through the terms describing interference effects between the wave functions of the different Stark components mixed by the constrained quadrupole interaction [23,24,33]

$$\phi^q_{n_1n_2m} = \frac{n}{2}\left[a_{k1}\sqrt{n_1\,(n-n_1)\,(n_2+1)\,(n-n_2-1)}\right.$$
$$\left. - a_{k2}\sqrt{n_2\,(n-n_2)\,(n_1+1)\,(n-n_1-1)}\right], \quad (16)$$

$$a_{k1,k2} = \frac{1}{e^2a_0^2}\,\langle n_1\mp1n_2\mp1m|\,\boldsymbol{d}\,|n_1'n_2'm'\rangle$$
$$\times\,\langle n_1'n_2'm'|\,\boldsymbol{d}\,|n_1n_2m\rangle^*, \quad (17)$$

$$\phi^\gamma_{n_1n_2m} = n^3\,(n_1-n_2)\,[(n-1)\,(|m|+1)+2n_1n_2], \quad (18)$$

where $\boldsymbol{d}$ is the dipole operator of the radiator. The corresponding expressions for the lower sublevel $n_1'n_2'm'$ are readily obtained from the written above three equations by the substitutions $\{n_1n_2m\}\longleftrightarrow\{n_1'n_2'm'\}$ [23,24,33].

The electron impact width of the individual Stark components is determined from the following equations the splitting between Stark sublevels being neglected [24,56]

$$\gamma_k^{(0)} = 3\sqrt{\pi}\frac{e^2}{\hbar\upsilon_e}(a_0^3N_e)M_k^\gamma L\omega_a, \quad (19)$$

$$M_k^\gamma = n^2\left[n^2+(n_1-n_2)^2-m^2-1\right]$$
$$+\,n'^2\left[n'^2+(n_1'-n_2')^2-m'^2-1\right]$$
$$-\,4nn'\,(n_1-n_2)\,(n_1'-n_2'),$$

$$L = \ln\frac{\rho_D}{\rho_W}+0.215,\quad \rho_D=\sqrt{\frac{T_e}{4\pi N_ee^2}},$$
$$\rho_W = \frac{n^2\hbar}{m_e\upsilon_e},\qquad \upsilon_e=\sqrt{2T_e/m_e}. \quad (20)$$

The reduced intensity of the Stark components is obtained within dipole approximation directly from Gordon equations [57] g_k being the statistical weight of the given component

$$I_k = g_k\frac{1}{e^2a_0^2}\,|\langle n_1n_2m|\,\boldsymbol{d}\,|n_1'n_2'm'\rangle|^2,$$
$$g_k = \begin{cases}1,\ m=m'=0\\ 2,\ m=m'\neq0\\ 4,\ m\neq m'.\end{cases} \quad (21)$$

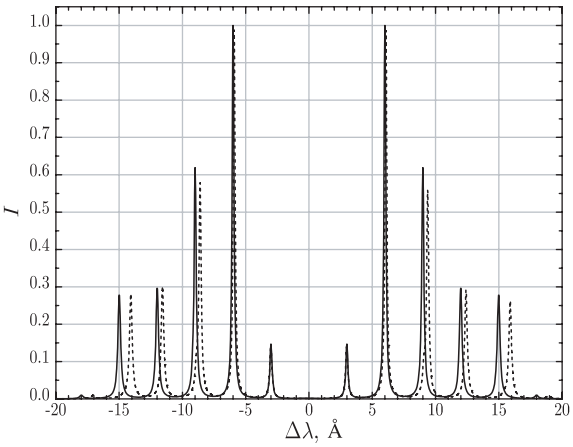

Fig. 3. Dependence of Stark component intensities versus wavelength detuning from line center at fixed value of ion microfield: solid line — linear Stark effect; dotted line — with constrained quadrupole interaction and QSE.

The ω_k^4 is not included conventionally in the above equation neglecting the Stark splitting of the levels that is approved by the structure of the general expression for the line profile [48,49]. The values of dimensionless quantities $\Pi_k^{(0)}$, M_k^γ, ε_k^{qs}, $\Delta_k^{qs}/(3/2)\Delta_k^d$, ε_k^q, $\varepsilon_k^{q\gamma}$, Δ_k^d, Δ_k^q for the different H_β components k are presented in Table 1. The QSE corrections to intensity and shift for various H_β components included in the table are evaluated using the data from [55].

It should be pointed out that for simplicity in the above formulae the hydrogen radiator and the perturber ions with the charge Z_p equal to unity are presumed. However, the scaling of these results on hydrogen-like radiators with the charge Z_r and complex composition of perturbing ions with $N_e=\sum_s Z_sN_i^{(s)}$ (Z_s is the charge of the perturbing ions with the partial concentration $N_i^{(s)}$) could be found in [33,34,52].

5 Influence of various sources on functional behavior of H_β line asymmetry

5.1 Fixed value of reduced ion microfield

Consider some aspects of dependences of the hydrogen atom spectral line H_β asymmetry functional behavior. In Figure 3 the dependence of H_β Stark components intensity is shown versus the wavelength for the fixed value of ion microfield for the linear Stark effect with account of the constrained quadrupole interaction (QI) and QSE and without account of the pointed out QI and QSE. As could be seen the account of QI and QSE changes the intensity and location of Stark components that leads to the asymmetry of the given line.

Table 1. Set of different broadening dimensionless parameters for H_β Stark components.

n_1n_2m	$n_1'n_2'm'$	$\Pi_k^{(0)}$	M_k^γ	ϵ_k^{qs}	$\Delta_k^{qs}/(3/2)\Delta_k^d$	ϵ_k^q	$\epsilon_k^{q\gamma}$	Δ_k^d	Δ_k^q
300	010	0.00020	496	2436	−197.143	−70	2.29032	14	−204
300	001	0.00319	392	1536	−230.333	−36	2.93878	12	−212
300	100	0.07197	304	812.843	−276	−2	3.84211	10	−204
201	010	0.00239	368	1172	−282.4	−34	4.13043	10	−44
201	001	0.07656	296	432	−353.5	0	5.18919	8	−52
201	100	0.11723	240	300	−470.667	6.57143	6.46667	6	−44
210	010	0.01615	304	−99.1111	−502.667	7.33333	2.89474	6	52
210	001	0.02871	264	−384	−755	20	3.39394	4	44
210	100	0.00179	240	−3396	−1508	118	3.8	2	52
102	001	0.15311	200	−160	−659	12	5.76	4	44
111	010	0.02871	240	−972	−1476	30	−0.066667	2	84
111	100	0.02871	240	972	1476	−30	0.066667	−2	84
120	010	0.00179	240	3396	1508	−118	−3.8	−2	52
120	001	0.02871	264	384	755	−20	−3.39394	−4	44
120	100	0.01615	304	99.1111	502.667	−7.33333	−2.89474	−6	52
012	001	0.15311	200	160	659	-12	−5.76	−4	44
021	010	0.11723	240	−300	470.667	−6.57143	−6.46667	−6	−44
021	001	0.07656	296	−432	353.5	0	−5.18919	−8	−52
021	100	0.00239	368	−1172	282.4	34	−4.13043	−10	−44
030	010	0.07197	304	−812.843	276	2	−3.84211	−10	−204
030	001	0.00319	392	−1536	230.333	36	−2.93878	−12	−212
030	100	0.00020	496	−2436	197.143	70	−2.29032	−14	−204

5.2 Asymmetry parameter

For the concrete calculations the density and temperature of plasma electrons are taken equal to $N_e = 1.36 \times 10^{17}$ cm^{-3} and $T_e = 13\,620$ K respectively that coincides with the conditions in stabilized arc precision experiments performed in Kiel University by the group of Helbig [9,13].

For study of the asymmetry of spectral line profile it is conventional to use the characteristic parameter of asymmetry $A(\Delta\lambda)$ that testifies the relative difference in the behavior of its red and blue parts [14,15]

$$A(\Delta\lambda) = \frac{I(|\Delta\lambda|) - I(-|\Delta\lambda|)}{I(|\Delta\lambda|) + I(-|\Delta\lambda|)}, \qquad (22)$$

where $\Delta\lambda = \lambda - \lambda_0$; c is the speed of light; $\lambda = 2\pi c/\omega$, $\lambda_0 = 2\pi c/\omega_0$ are the perturbed and unperturbed wavelengths of the line. In some papers the definition of $A(\Delta\lambda)$ differs from the given above (22) by factor of 2. Moreover, it is important to state with respect to what reference point the detuning $\Delta\omega$ is defined. In this work it is assumed that $\Delta\omega$ is taken with respect to the unperturbed line center ω_0. However, in [14,15,37] were introduced other asymmetry parameters differing by the definition of reference point and by transcendent dependence from detuning value, and to some extent adminicular to each other.

5.3 Trivial asymmetry

Before to proceed to analysis of contributions from the different interactions entering the asymmetry parameter pay attention on the "trivial asymmetry", connected first of all with the transition from the cyclic frequency scale to the wavelength one [14,15,42]. So, for H_β line having the record broadening value this effect turns out to be very significant. In Figure 4 the arising and changing of asymmetry of initially symmetric H_β Stark profile due to two factors of trivial asymmetry — expressing of the frequency through the wavelength and the Jacobian of conversion of the frequency scale into the wavelength one — is consistently represented.

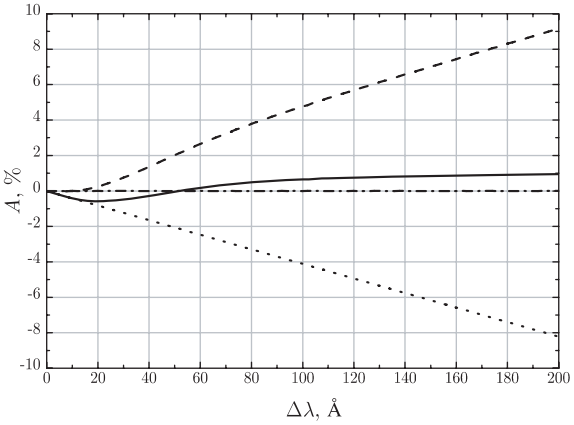

Fig. 4. Comparative behavior of $A(\Delta\lambda)$ for H_β line due to different factors of trivial asymmetry: dash-dotted line — without account of trivial asymmetry factors; dashed line — transition from the frequency to the wavelength in argument; dotted line — Jacobian of conversion from the frequency scale to the wavelength one; solid line — complete account of trivial asymmetry.

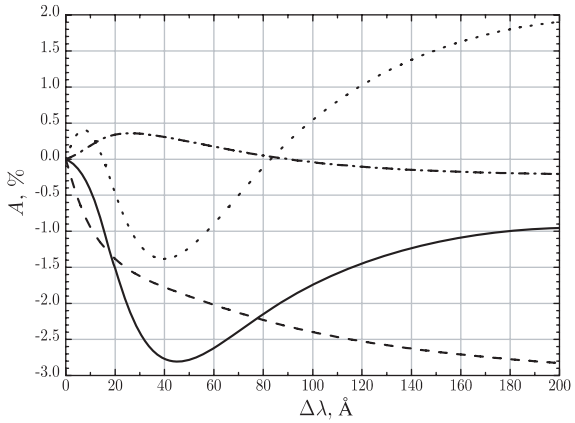

Fig. 5. Dependences of H_β line $A(\Delta\lambda)$ due to influence of quadrupole interaction: dotted line — correction to shifts of Stark components; dashed line — correction of Stark component intensities; dash-dotted line — correction of impact electron widths of Stark components; solid line — complete correction due to QI.

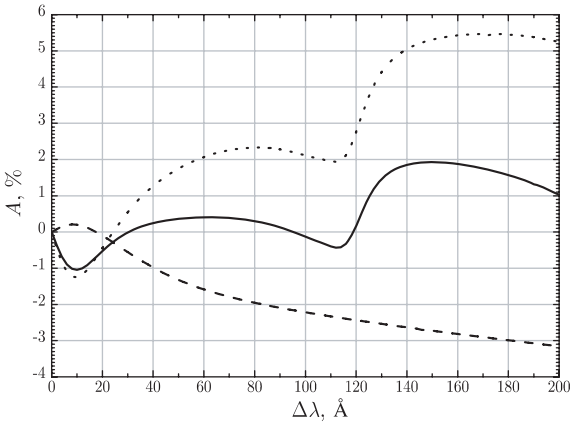

Fig. 6. Dependences of H_β line $A(\Delta\lambda)$ due to induced by QSE influence on Stark components intensities and shifts (proportional to square of reduced ion microfield): dotted line — correction of Stark components shift only; dashed line — correction of Stark components intensities only; solid line — complete correction due to QSE.

As it is seen in this figure the contour that is initially symmetric in frequency domain after transition to wavelength domain exhibits monotonous "red" (positive) asymmetry with the increase of the detuning from the line center.

The Jacobian of conversion on the contrary induces the blue (negative) asymmetry of the initial contour, that is also increasing with the increase of detuning. The joint action of both factors leads as to the significant reciprocal compensation of contributions as to the complex functional behavior of "trivial asymmetry" with the change of its sign versus the detuning value.

The role of trivial asymmetry may be demonstrated on the following example. Indeed, the asymmetry parameter for H_β line due to quadrupole interaction is negative for any frequency in the frequency scale, that does not fit the experimental positive sign of asymmetry (red asymmetry) in the wavelength scale. But if to represent the intensity in the frequency scale as the function of the wavelengths the asymmetry parameter sharply increases and becomes positive beyond localizations of H_β line peaks, that by the behavior pattern corresponds to the upper curve in Figure 4. Note that namely in this settings the tabulation of profiles was done in [30].

5.4 Constrained quadrupole interaction

Setting the trivial asymmetry aside for the moment consider the asymmetry parameter (22) behavior versus wavelength for Holtsmarkian distribution of ions microfield $W_H(\beta)$ [53] under inclusion of the quadrupole corrections, given by equations (5–18). The main part of calculations presented here (unless otherwise stated) are performed with $W_H(\beta)$ and $B(\beta)$.

As it is seen in Figure 5 the least contribution is given by the correction to the electron impact halfwidth, and the largest one by the correction to the intensity, which has blue asymmetry, and that is why the resultant curve with account of all quadrupole corrections also has the blue asymmetry.

5.5 Quadratic Stark effect pattern

In Figure 6 the comparison of asymmetry behavior under the QSE [55] influence on intensities δ_k^{qs} and shifts s_k^{qs} of Stark components in (5)–(18) is shown. In previously published articles the QSE influence on intensity values of Stark components was unsoundly neglected [26,32,36,39].

In the region $\Delta\lambda > 25$ Å the correction to intensity has blue asymmetry, while the correction to the shift has red asymmetry. In the range of $\Delta\lambda < 20$ Å the situation becomes completely opposite. The resultant dependence has extremum in the range of 110–120 Å [22], that is due to the QSE correction to the shift. The appearance of such type of extrema was noticed earlier in [14,42,44] as well as in [32], where its origin was not analyzed.

5.6 Joint action of constrained quadrupole interaction and quadratic Stark effect

In Figure 7 the dependence of asymmetry versus the wavelength with account of the constrained QI and QSE is shown.

It is seen that QSE gives noticeable contribution into asymmetry behavior that is comparable with QI. The resultant curve with account of both interactions has extremum already in the region 150–160 Å. However, in the case of earlier investigations using perturbation theory as in [14,42], the extremum is localized at smaller values of detunings, that is the evidence of noticeable competition of interactions in resolvent and non-linear character of its eigenvalues dependence on the reduced microfield value, i.e. the effective values of β giving the main input in the integral (4) over all ion microfield values.

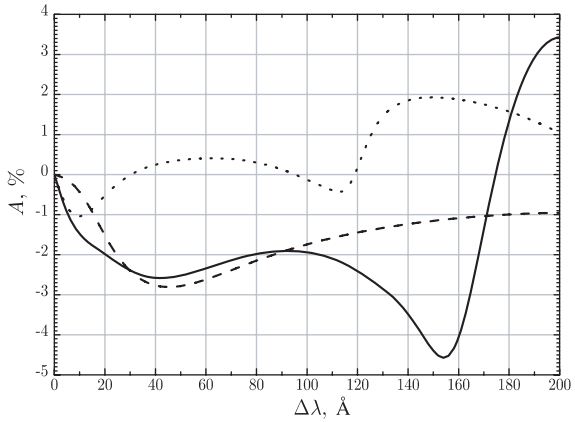

Fig. 7. Comparison of H_β line $A(\Delta\lambda)$ behavior with account of QI and QSE: dashed line — only QI contribution; dotted line — only QSE contribution; solid line — summary contribution of QI and QSE.

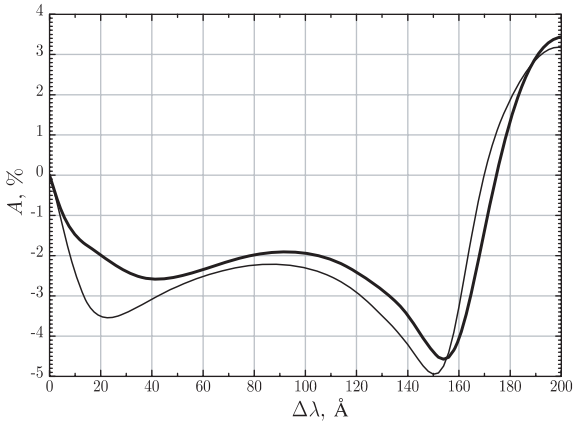

Fig. 8. Comparison of H_β line $A(\Delta\lambda)$ against ion microfield distribution function: thin line — nearest neighbor; solid line — Holtsmark.

5.7 Influence of the type of microfield distribution

In Figure 8 the comparison of asymmetry calculated on the basis of the two different microfield distribution functions is presented.

It is seen that the general trends of the curves behavior practically coincides with each other for the NN and W_H distributions. Only in the range of $\Delta\lambda \sim 20$ Å one can see the significant deviations.

5.8 Inclusion of trivial asymmetry in general scheme with details for each Stark component

To this moment the contribution of the trivial asymmetry was not considered and the frequency was recalculated into the wavelength according to the linear law

$$\frac{\Delta\omega}{\omega_0} \approx -\frac{\Delta\lambda}{\lambda_0}. \tag{23}$$

For small detunings $\Delta\lambda \ll \lambda_0$ the approximation (23) gives satisfactory results for the resultant profile. But the influence of trivial asymmetry as it was shown above is significant (compare with [14,15]). For correct conversion of argument from the frequency scale into the wavelengths it is necessary instead of (23) to use expression

$$\frac{\Delta\omega}{\omega_0} = -\frac{\frac{\Delta\lambda}{\lambda_0}}{1+\frac{\Delta\lambda}{\lambda_0}}. \tag{24}$$

The account of the transformation of variables Jacobian according to (24) leads to the following connection of the intensity in the frequency scale with intensity in the wavelength scale:

$$I(\Delta\lambda) = \frac{2\pi c}{\lambda_0^2}\frac{I(\Delta\omega)}{\left(1+\frac{\Delta\lambda}{\lambda_0}\right)^2} \tag{25}$$

with $\Delta\omega$ defined from (24). The joint influence of the both trivial asymmetry factors under correct transition from the frequency scale to wavelengths is shown in Figure 9.

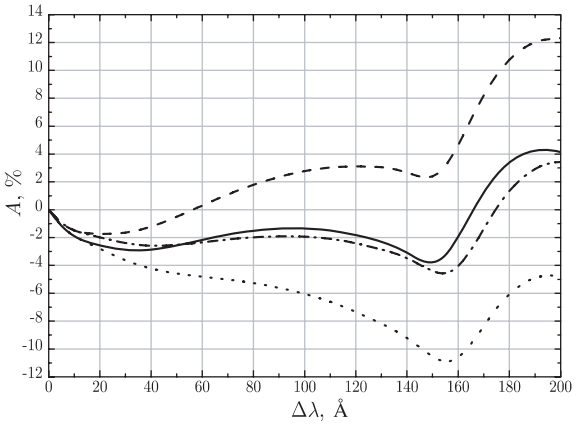

Fig. 9. Influence of transition from frequency scale to wavelength one on H_β line $A(\Delta\lambda)$ behavior with account of QI and QSE: dash-dotted line — without account of trivial asymmetry factors; dashed line — transition from the frequency to the wavelength only in argument; dotted line — only Jacobian of conversion from the frequency scale to the wavelength one; solid line — complete account of trivial asymmetry.

According to the performed above analysis the transformation of argument to wavelengths (24) gives the red asymmetry, and the transformation of intensity (25) gives the blue asymmetry. The curve corresponding to simultaneous account of all considered sources of asymmetry together with trivial asymmetry almost repeats the shape of the curve obtained without account of influence of transition to wavelengths. The comparison of contributions of each Stark component of the line during the transition to the wavelength scale is shown in Figure 10. The main input is due to the components with larger intensity $\Pi_k^{(0)}$.

5.9 Influence of electron collision shifts

As it was demonstrated in [14,42,44] $A(\Delta\lambda)$ for small detunings near the center of the line is a very sensitive function of the values and signs of individual Stark components

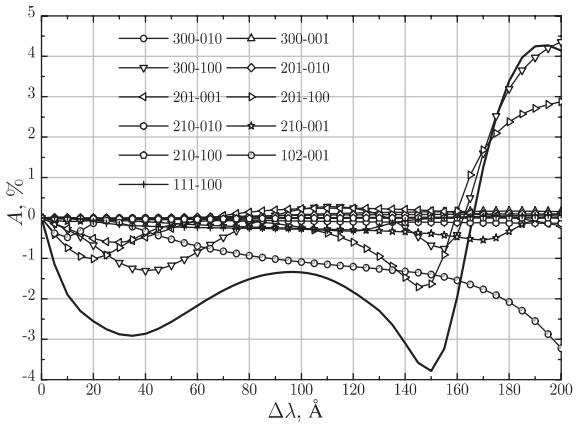

Fig. 10. Influence of individual Stark components contributions on H_β line $A(\Delta\lambda)$ behavior: solid line — $A(\Delta\lambda)$ of H_β total profile.

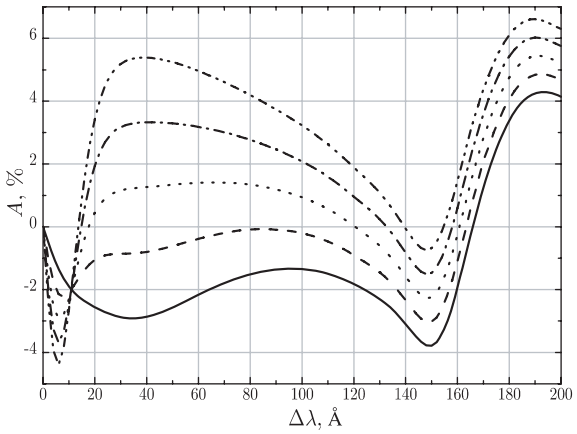

Fig. 11. Influence of individual Stark components electron collision shifts values on H_β line $A(\Delta\lambda)$: solid line — no electron collision shifts; dashed line — the electron collision shift of any component is $d_k^{(e)} = 0.5$ Å; dotted line — $d_k^{(e)} = 1.00$ Å; dash-dotted line — $d_k^{(e)} = 1.50$ Å; dash-double dotted line — $d_k^{(e)} = 2.00$ Å.

electron collision shifts [32,36,39,47]. In Figure 11 the deviation of $A(\Delta\lambda)$ versus $\Delta\lambda$ for the set of arbitrary taken and mutually identical values of red shifts for each Stark component of the H_β line is presented, that illustrates these peculiarities of functional asymmetry behavior.

For the further test the electron collision shifts calculated in [58] within Green function formalism [32,36,59] were taken, that happens to be approximately equivalent to the identical shift of each Stark component to the red about 1 Å, and thereby to the overall shift of the whole line approximately of the same value (see Fig. 12).

It is important to underline the qualitative and quantitative strong influence of the introduction of electron collision shifts on the cross-over point location, where the $A(\Delta\lambda)$ changes its sign, and on the location, sign and shapes of its extrema. It is seen that the appearance of the cross-over point occurs for the some $d_k^{(e)}$ values that are greater or equal to some critical value. Above this critical value under further increasing of $d_k^{(e)}$ there is definite similarity in the behavior of $A(\Delta\lambda)$ curves.

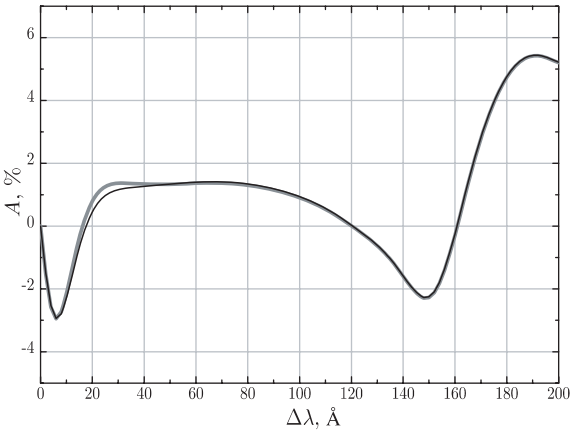

Fig. 12. Behavior of H_β line $A(\Delta\lambda)$ versus the way of electron collision shifts introduction: dashed line — the different values of electron collision shifts of Stark components, generated within Green function approach [58]; solid line — the equal electron collision shifts for all Stark components of line.

5.10 Details of extrema due to quadratic Stark effect shifts

Now it is useful again to reconsider the behavior of $A(\Delta\lambda)$ in Figure 13 with more ample representation of the different Stark components extrema after the introduction of the electron collision shifts $d_k^{(e)}$ [58]. The extremum around 150 Å is due to transition 201–100, at about 200 Å due to transition 102–001, and at about 250 Å — due to transition 201–001 etc. These extrema are due to the dominating contribution to the Stark components QSE shift in the resolvent. The changes of the extrema shapes in Figure 13 are obvious in comparison with Figure 10, where the electron collision shifts are not entered. In Figure 13 the extrema are more pronounced, namely, relatively more narrower and deeper.

5.11 Boltzmann and dipole intensity scaling factors

There are two more factors that were earlier considered under asymmetry calculations, for example, by Griem [19], who used though only the first order expansions of these factors over small parameters. The first of them is the multiplier ω^4 that is due to scaling of dipole radiation and neglected under consideration of symmetric line shape [48,49]. The second one is the exponential Boltzmann factor, introduced to satisfy Kirchoff law at any current frequency value [48–50]. After that the intensity is assumed to be proportional to pointed above factors:

$$I(\Delta\omega) \sim \left(1 + \frac{\Delta\omega}{\omega_0}\right)^4 \exp\left(-\frac{\Delta\omega}{T_a}\right), \qquad (26)$$

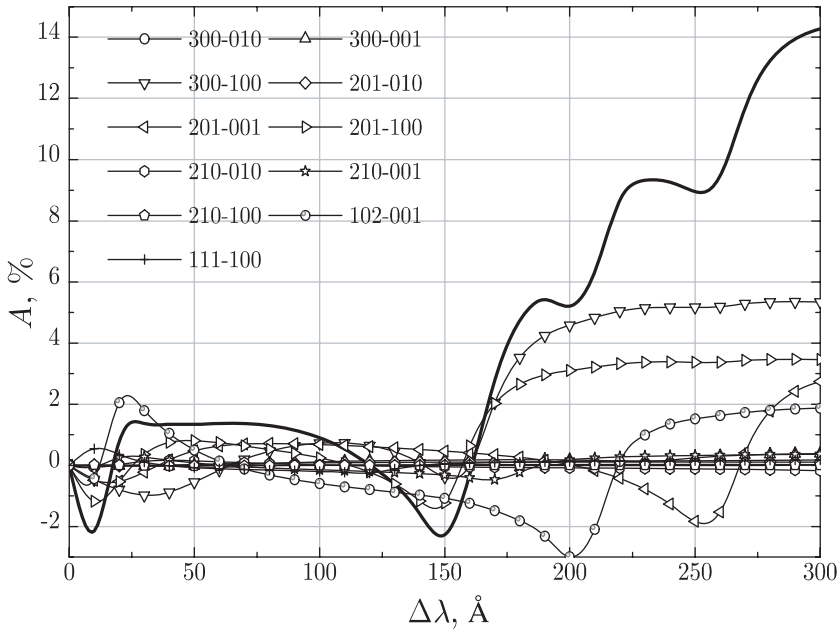

Fig. 13. Comparison of $A(\Delta\lambda)$ extrema shapes and their localizations, induced by QSE shifts, after introduction of the individual electron collision shifts for the different Stark components of H_β line [58]: solid line — $A(\Delta\lambda)$ for the total H_β line profile.

where T_a is the effective temperature equivalent to the Boltzmann distribution for population of the considered quantum levels with principal quantum numbers $n = 4$ and $n = 2$ of hydrogen-like atom. Conventionally in the stabilized arcs the existence of LTE is assumed and $T_a \approx T_e$ is expected [2,3,7].

However, the direct introduction of the above equation in the contour calculations would lead to the exponential divergence at the infinite negative detunings in frequency scale from the line center as was already pointed out in [14,15].

At the positive detunings in frequency scale from the line center there would be no divergence due to the exponential decrease of the Boltzmann factor that is stronger than the power increase of ω^4 [4]. Thus as was already discussed in [14,15,42,44] to progress further one needs to limit the range of the contour definition only by the negative detunings $\Delta\omega = \omega - \omega_0$ that lie inside positive frequency domain i.e. $\omega \geq 0$. Secondly, it is necessary then to reconsider the normalization conditions of the redefined contour that includes now the above discussed factors (see [14,15,42,44]). In the following, Figure 14 illustrates how ζ, being the deviation from unity of the normalization constant for the redefined contour, depends on the effective excited levels population temperature values. It is seen that in a wide range of T_a changes the correction to normalization is less than about 1.5%. Moreover, it is more important that these deviations of normalization constant would not influence asymmetry anyway.

The characteristic behavior of $A(\Delta\lambda)$ for additional inclusion of these factors with corresponding necessary redefinitions of the contour (see [14,15,44]) is represented in Figure 15 for $T_a = T_e$.

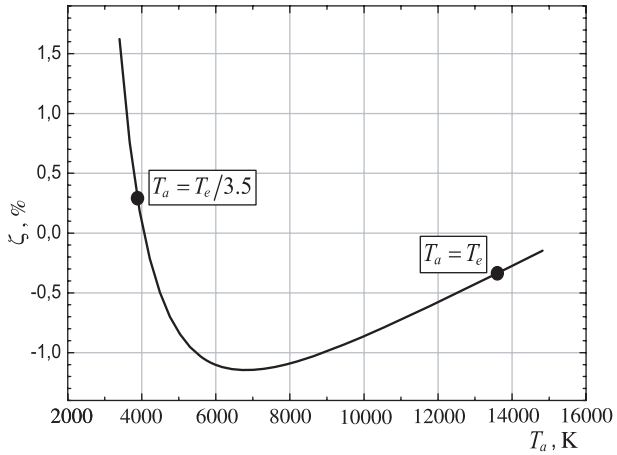

Fig. 14. The deviation of H_β contour normalization constant ζ from unity in percents due to the introduction of the intensity scaling factor ω^4 and the Boltzmann factor versus the effective excited levels population temperature value T_a for $N_e = 1.36 \times 10^{17}$ cm^{-3} and $T_e = 13\,620$ K.

As it is seen the account of exponential factor leads to the red asymmetry, and the account of ω^4 multiplier — to the blue one. As a rule $T_a < T_e$, and that is why the joint action of both factors could give deviation as to the red side, as to the blue one (see [14,15,44]).

It should be noted that in the previous works [31,32,36,39] that claimed inclusion of ω^4 and Boltzmann factors corresponding to the electron temperature T_e beyond the first order perturbation approach over $\hbar\Delta\omega/kT \ll 1$ and $\Delta\omega/\omega_0 \ll 1$ strangely no explanations concerning the divergence for the negative detunings in the frequency scale were given.

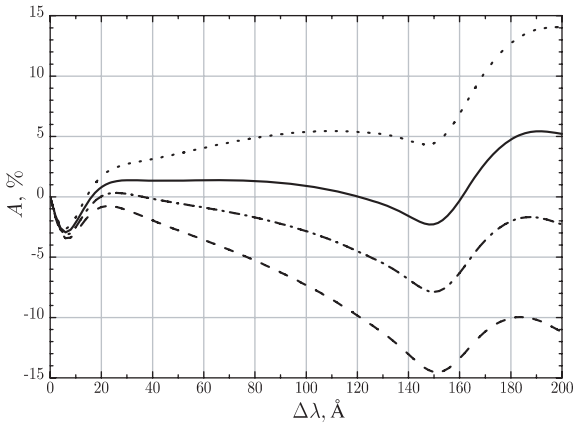

Fig. 15. Influence on $A(\Delta\lambda)$ due to the introduction of the intensity scaling factor ω^4 and the Boltzmann factor, corresponding to the electron temperature value: solid line — without intensity scaling factor ω^4 and Boltzmann factor; dashed line — only with intensity scaling factor ω^4; dotted line — only with Boltzmann factor; dash-dotted line — joint inclusion of intensity scaling factor and Boltzmann factor.

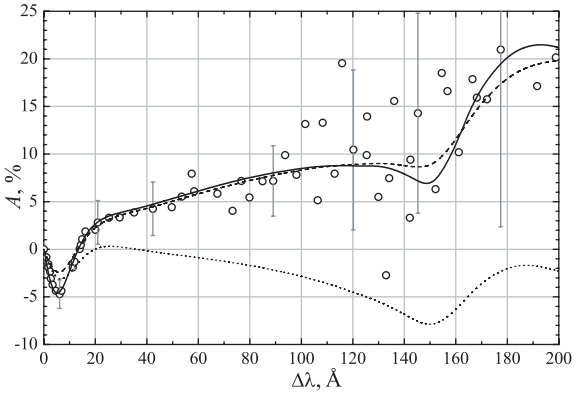

Fig. 16. Comparison of experimental measurements of H_β line $A(\Delta\lambda)$ with different versions of theoretical computations: empty circles — experiment [13]; dotted line — with inclusion of intensity scaling factor ω^4 and Boltzmann factor for atomic levels effective population temperature $T_a = T_e$; dash-dotted line — with inclusion of intensity scaling factor ω^4 and Boltzmann factor for the effective atomic levels population temperature $T_a = T_e/3.5$; solid line — with inclusion of intensity scaling factor ω^4 and Boltzmann factor for atomic levels effective population temperature $T_a = T_e/3.5$ and the reduced by factor 1.4 the electron impact width. The uncertainty associated with experimental results has been adopted from [14], details of which may be found in [13].

5.12 Comparison with experiment

The comparison with experimental data obtained for H_β emission line of atomic hydrogen in the stabilized arc in the group of Helbig at Kiel University ($N_e = 1.36 \times 10^{17}$ cm^{-3} and $T_e = 13620$ K [9,13,14]) is shown in Figure 16 (see also [44]). The experimental setup was similar to one given in [9], where the electron density was measured by the independent interferometric methods. Since the bulk of ions are Ar^+ [9] the implementation of quasistatic approximation for description of ion broadening is rather well justified. In distinction from the conventional assumptions the temperature of electrons T_e and the effective excited levels population temperature T_a are allowed to differ here, and namely for the satisfactory fitting of the calculated curve to the experimental points it was chosen $T_a = T_e/3.5$. As was reported earlier (see [14,15]) the theoretical curves based on the perturbation theory in the contour provided for $T_a = T_e$ exhibit unsatisfactory agreement with experimental data and this is confirmed by the present non-perturbative results in Figure 16 for this case. As a whole this section analysis is further development of the ω^4 and Boltzmann factors consideration, performed in [14,15,42]. The calculations take into account consistently as was described in the previous sections the constrained quadrupole interaction, the quadratic Stark effect, the electron collision shifts, the conversion to wavelength scale, the ω^4 and Boltzmann factors (26) with the necessary redefinitions of the contour.

One can see that for $T_a = T_e/3.5$ the performed comparison shows the satisfactory agreement but the value of the trough in the range ∼5 Å is less than experimental one. Partly, this is connected with the diagonal approximation, ignoring the non-diagonal matrix elements of electron impact broadening operator and as consequence the line narrowing near the center due to redistribution of intensities between Stark components [24,56]. That is why the diagonal approximation leads to some overestimation of the effective electron impact broadening values [24,56,15]. Indeed, as seen from comparison in Figure 16 for the reduced value of electron impact widths by factor 1.4 the quality of trough fitting becomes much better while in the outer regions this does not make worse overall agreement with experimental points. It is worthy to draw attention to the comparison of the first extremum localization due to QSE shift and the range of strong scattering of experimental points and minimum of experimental data in the range of 140–180 Å, that probably would bid further detailing and more fine and accurate measurements. Also pay attention that as it is seen in Figure 16 under reduction of the electron impact widths the extrema due to QSE are evinced more patently. It is very important to note that the sound fit of the cross-over point location of $A(\Delta\lambda)$ is possible only due to the introduction of the electron collision shifts of the certain values of the order of about 1 Å (compare [14,44]). *This feature thus provides the unique possibility of indirect verification of the electron collision shifts values against experimental measurements!*

6 Discussion

6.1 Non-perturbative and perturbative approaches in the contour

First of all it is important to note that the presented above detailed non-perturbative results (with respect to the absence of perturbation expansion in the contour over the quadrupole interaction, see also [44]) in their main trends

coincide with the earlier obtained results of perturbation theory [42]. In both approaches the same consistent consideration of QSE was applied [14,15,42]. Of course, details of asymmetry extrema in the non-perturbative theory as well as the character of competition of various asymmetry sources experience deviations in comparison with perturbation approach [14,15,42]. Indeed, if within the perturbative approach the considered corrections are additive, in the non-perturbative case the various corrections compete with each other in non-linear way.

6.2 Standard theory

In general this work utilizes the so-called Standard Theory (ST), or Conventional Theory (CT) settings [48,49]. Namely this imply the quasistatic ion microfield and the electron impact broadening. But due to appealing for joint action of microfield and its derivatives the constrained quadrupole interaction influence on intensities, frequency shifts and electron impact widths together with the QSE influence on intensities and frequency shifts [14,15,23] are included. Again the diagonal approximation for the electron impact broadening operator and the no quenching approximation are used for the electron impact widths calculations [24,56], while the electron collision shifts are taken from the different approach, developed in [31, 32,36] and based on the kinetic Green functions technique [59]. The microfield distribution function is taken to be Holtsmarkian [48,49]. At the same time the parabolic wave functions set is taken for the zero approximation wave functions [54–57]. The latter in conjunction with the mentioned above diagonal approximation leads to some overestimation of the electron broadening in the center of the line where the effective electron broadening is narrower due to the electron broadening operator non-diagonal matrix elements [24,56]. Thus in comparison with ST results [48,49] the described procedure overestimates the broadening due to ions and electrons within the settings of ST [15]. This is one of the reflections of the important general thesis stated earlier in [23,24,30], that for the asymmetry analysis it is necessary to perform calculations of the total contour on the contrary to what was argued and done in earlier works (see [19–47]). *And this illustrates the unforeseen previously circumstance that the asymmetry is the fundamental multiparameter dependent sensitive function of broadening mechanisms affecting the Stark profiles of hydrogen spectral lines [14,15,42,44], and in particular strongly dependent on the choice of the reference point [14,15].* It is worthy to point out the better agreement with considered above experimental results for the reduced by factor of 1.4 the impact electronic widths of Stark components towards the lesser electron density range in accordance to the discussion and arguments given above and more detailed results presented in [42,44]. Indeed, it was noticed earlier that the quasistatic binary profile asymmetry along with settings of Kudrin and Sholin for the quadrupole H asymmetry [18] is strongly damped by the introduction of the impact electron broadening just due to renormalization [23]. Thus the decrease of the impact electron broadening leads to the increase of asymmetry [44], while the dip between peaks becomes more pronounced [48,49]. The dependence of the dip on the character of electron broadening in particular was the reason for judging that the ion dynamics is not so important, but the electron broadening should be described in the better theoretical approach than the impact approximation [60]. To be fair it should be noted that the presented here "logarithmic" approximation for the expression of the impact width is simplified version of the more general results containing the influence of the Stark splitting between the sublevels in the ion microfield [24, 56]. The increase of this splitting leads within this more general approach to the additional decrease of electron impact widths and shifts [24,56].

There is also the empirical cut-off procedure [61] redefining the expression for logarithm accounting to the effect of incomplete collisions and introducing competition between the detuning from the line center, the splitting in the ion microfield and the electron plasma frequency, that somehow decrease the impact widths. Additionally more rigorous approaches going beyond the perturbation theory for the impact width also should predict the narrowing of electron broadening of Stark components (see [62] and reference therein).

However, for the moment all these complications are supposed to give more fine structure for already considered dependences and could be analyzed further elsewhere.

6.3 Dynamical theory

Besides the theory of Stark profiles asymmetry that could be classified as ST with respect to the impact electrons and quasistatic ions broadening, the dynamical approaches (DA) were developed [37,39,41,46]. The recent DA version is based on the simultaneous simulation of time evolution of both the electric fields of ions and electrons using only the dipole approximation for the interaction potential and the straight trajectories path approximation [46]. First of all in principle the latter version of DA [46] should provide more correct and ample description of the electron broadening in comparison with the impact approximation, and the ion broadening in comparison with the quasistatic approximation [48,49]. Moreover, the further solution of time dependent Schrödinger equations for the wave functions evolution operators is obtained [46] as some analog of the close coupling approach in the theory of atomic collisions (see [48]) considering at once all states belonging to the principal quantum numbers from 1 to 5. The quadrupole interaction was omitted in these calculations and only the dipole interaction with dynamic microfields is retained. The final profile is obtained with the help of interaction representation and the some kind of rotating wave approximation [46].

However, on the basis of obtained DA results [46,51] it is still difficult to judge on the significance of the electric fields dynamics influence on the hydrogen Stark profile asymmetry. Indeed, it was known that ion dynamics mostly affects the dip located about the line center and

makes it less deep [4,7,51]. In the region of halfwidth the H_β Stark profiles were found practically insensible to ion dynamics, that allows to use the quasistatic estimate of the HWHM as the tool to diagnose the ion density in plasmas for almost 88 yeas since the work of Holtsmark [51]. The special efforts in attempt to find experimentally some correlations between asymmetry and ion dynamics effects gave also the negative answer [8]. So, on these grounds it would be sound to presume that the ion dynamics is ineffective for detunings larger than the HWHM.

But the consideration of the pure quadrupole interaction within such DA version would give in particular the tool to diagnose the existence of the quasistatic limit in the line wings and the character of conversion to it from the impact limit [24,33]. Indeed, the cancellation of the quadrupole contributions of ions and electrons while stemming to the quasistatic limit could be used for testing the behavior of this transition [33,48,49]. At the same time the contributions from the quadratic Stark effect would stem to be doubled due to addition of the ion part to the contribution from electrons as far as the conversion to quasistatic limit would occur [48].

Regrettably, the described important effects were not studied yet in the presented dynamic results [46] first of all because the quadrupole interaction was neglected. Moreover, it appears that the expectations of [40] toward the exact treatment of quadrupole interaction within this version of DA [46] are at present no more than delusions. Indeed, this obviously is not any simpler than construction of joint distribution functions due to appearance of the additional "time" variable. For each separate trajectory DA procedure is based on the binary notions but in the next step one have to generate the evolution history. Any additional variables like the electric field derivatives would only increase complexity and likely prohibit further computational efforts even with the use of clustered technology deployed in [41]. However, since the dynamic results give lesser electron broadening the DA asymmetry should better describe the experiment when compared to the crude fitting within ST simply by decreasing the effective electron widths values [16].

The H_β asymmetry in [46] does not have any extrema although this study shows it should be induced by the static QSE. On one hand those extrema could disappear due to the dynamical picture of interactions or due to the additional smoothing procedures applied in simulations to reduce the noise. On the other hand averaging over all directions in simulations could also lead to the same result. Moreover, those extrema are located at detunings corresponding to the rather far line wings that probably could not be described with sufficient accuracy by this simulation method.

The important additional difference between the DA [46] and the present ST approach is that it uses the basis of spherical wave functions, and does not operate explicitly with the notion of Stark components. Moreover, it is unclear how completely the DA includes the contribution to asymmetry from the electronic collision shifts. Indeed, the DA [46] seems to incorporate the "dynamic" analog of inelastic collisions between the levels with $n, n' = 1 \div 5$, but ignores the recoil effects due to straight trajectories in simulations. So, the latter important source of the electron collision shifts [47] remains unaccounted in the DA [46] model. On the other hand the "dynamic" inelastic collision shift could differ considerably from the corresponding results of [47]. Meanwhile, in the present ST settings the electron collision shifts are introduced on the basis of the additional consideration exploiting Green function formalism [32,59]. Also for the experimental conditions under discussion there is no point to consider any possible "dynamic" ion collision shift contribution.

There were also other attempts to calculate the asymmetry of Stark profiles of hydrogen spectral lines using less consistent schemes for description of temporary dynamics of microfields in plasmas like using Model Microfield Method (MMM) for both ion dynamics and the electron broadening [37,38], or simulation of the ion dynamics and adopting the impact broadening for electrons [39].

It should be noted that the method of simulations along straight trajectories, firstly applied for calculations of Stark profiles in [63,64], in the case of ion radiators should be replaced by the Method of Molecular Dynamics (MMD) due to the strong interaction of the charged perturbing particles between each other and with the radiator [65].

6.4 On accessibility of quasistatic limit for electrons

In order to judge on necessity of DA application for the description of H_β broadening by electrons it is useful to estimate the wavelengths corresponding to the Weisskopf frequency for broadening by electrons for the different Stark components of the line [48]. This could be done conventionally only for the interaction potentials proportional to R^{-L}, where R is the distance between particles and L is the positive integer [48]. Thus choosing for this the leading part of the potential — the dipole interaction — one could obtain characteristic scales of detunings from the line center up to which the impact approximation is valid, and beyond which — the quasistatic one [48,49]. The calculations are done for the mean values of electron velocities v_e using expressions (20). In fact these frequencies correspond to transition from impact to quasistatic regimes of broadening, the both of these limiting descriptions being invalid. In other words these frequencies are intermediate when under further increase of frequency (or wavelength) detunings the impact mechanism is interchanged by quasistatic one. These results are presented in Table 2, where the Weisskopf detuning in the wavelength scale for dipole interaction is designated by $\Delta\lambda_W^d$. As it is seen from these data for all H_β Stark components the conditions of impact approximation validity are fulfilled in the range of experimentally measured detuning from the line center.

However, starting already from $\Delta\lambda > 200$ Å for some components it is necessary to account for electron quasistatic broadening. Nevertheless, as was already stated

Table 2. Values of Weisskopf wavelength detunings $\Delta\lambda_W^d$ for dipole broadening induced by electrons for each H_β Stark component at $T_e = 13\,620$ K.

n_1n_2m	$n_1'n_2'm'$	$\Delta\lambda_W^d$ Å
300	010/001/100	213/248/298
201	010/001/100	298/373/497
210	010/001/100	497/745/1491
102	001	745
111	010/100	1491/1491
120	010/001/100	1491/745/497
012	001	745
021	010/001/100	497/373/298
030	010/001/100	298/248/213

above the main contribution to asymmetry and line profile is given by more intense Stark components, for which the range of conventional validity of the impact approximation for electrons is larger than the maximum experimental detuning value of 200 Å from the line center, while the components with small intensity could be neglected. At the same time, as contributions of electrons and ions from quadrupole interaction are compensated in the case of the same broadening regimes whereas summed up for QSE, the study of joint dynamical description of electron and ion broadening is an outstanding problem [33,37].

6.5 Complementary asymmetry sources

Besides the quadratic Stark effect there are other contributions of the same order such as the second order quadrupole corrections to the wave functions and the octupole corrections to the frequency and wave functions [20,23]. Nevertheless, the consideration restricted in this order by only the quadratic Stark effect has its own merits [44]. Moreover, additionally the non-ideality effects of particle interactions in plasmas [26–29,31,34,37], the fine structure splitting [57], the dissolution effect in strong microfields [27,57] are known to cause the asymmetry and were not included in the presented calculations. It is worthy to note that the results of DA approach [46] are obtained with the partial account of non-ideality effects with the help of introduction of Debye screening separately for the electron and ion electric fields [46], which also contributes to deviations from results of ST theory established with the Holtsmark microfield distribution function (MDF).

In principle the latter plasma coupling effects could be easily introduced in the considered ST scheme by using the Hooper's or Baranger-Mozer MDF [52]. Moreover, the Baranger-Mozer formalism introduced and analyzed for plasma with the complex ionization composition was already elaborated in [24,28,29,33–35] (compare with [31]) addresses the present ST consideration of asymmetry effects that consistently account for plasma coupling. In [24,28,29,33–35] the MDF and the first moments of microfield non-uniformity tensor include the electron Debye screening of ion microfields, the ion-ion correlations and the plasma polarization effects. The last one contribution arises due to the overall plasma quasi-neutrality condition [24,28,29,33–35]. Meanwhile, the preliminary asymmetry calculations within the above depicted procedure performed recently [45] showed insignificant changes in comparison with presented here results (without contribution of the polarization interaction [28,29,33–35]).

Therefore the further consideration of the plasma coupling and polarization effects (within introduced in [24,28] Baranger-Mozer formalism, for example) as well as other asymmetry sources pointed out here in ST and DA would be necessary.

6.6 Electron collision shifts and deviation of electron and population temperatures

Under stated assumptions, the developed approach endures satisfactory description of experimental results. In fact, the implemented electron collision shifts are obtained beyond the conventional impact approximation. They contain two parts, one of which describes transitions to levels with the different values of principal quantum numbers thus representing itself contribution outside of the no quenching approximation [47]. The other part goes beyond the classical path approximation by taking account of recoil effects for electrons in scattering process [47], and corresponds to $\Delta n = 0$ transitions. The implementation of fitting procedure for values of the electron collision shifts at the present stage is justified due to incompleteness and ongoing debate on the current status of the theory of these effects [66].

Indeed, besides the ST theory recently was created similar but differing approach — the so-called GT (Generalized Theory) and AGT (Advanced Generalized Theory) [66]. Presently there is a debate between results of the ST theory and the ones of GT and AGT, whose recent developments [66] are yet to be understood and interpreted in community.

The GT and AGT [66] exploits the method used in [56] of dressing the atomic states by ion microfield. However, the electric fields of plasma electrons in distinction from [56] are divided in two parts parallel and perpendicular to the ion electric microfield strength vector [66]. These two parts are then considered separately: the parallel contribution by using adiabatic non-perturbative approach, and the perpendicular one by using the perturbative expansion up to the second order like it was done in ST [48,49,56]. Such separation is, in fact, typical in the theory of magnetic resonance, laser physics etc., and is based on the general notions of slow and rapid perturbations. However, in the magnetic resonance the parallel and perpendicular magnetic fields often have different physical origin, while in GT and AGT there is a perplexing point due to the fact that the both components originate from the electric field of one electron.

But this setting alone invokes drastic changes in the important theoretical predictions [66]. For example, the so-called broadening widths and shifts functions $A(z)$ and

$B(z)$ (see [24,48,49]) in AGT become redefined and parametrically dependent on the microfield value [66], and start to oscillate versus the impact parameter as opposed to monotonic behavior of their analogs in ST [24,56]. However, in comparison given in Figure 4.1 in [66] one can find rather unusual negative values for $A_{-}^{\mathrm{AGT}}(z)$ in the range of small values of impact parameter. One additional AGT feature is that the electronic impact shifts obtained within the dipole approximation for the interaction potential in the no quenching approximation become nonsymmetric contrary to ST [56] and changing their sign versus the change of the microfield value [66,67]. The total electronic collision shifts thus become more complex — and related to the sum of contributions considered by Griem and the several contributions derived in the frames of GT and AGT [66].

From one side the appearance of adiabatic terms in the impact theory could be only welcomed, since their absence was a long-standing methodological drawback in the derivation of the impact approximation. But on the other side it is evident that AGT should also have some bounds not yet established for the small values of ion microfield where the exploitation of the dressed states representation is no longer valid.

The implementation of AGT results in the total Stark profiles calculations necessary for asymmetry analysis at the moment seems rather difficult and premature. This is mainly due to the complicated behavior of the AGT broadening functions and the complex competition of several mechanisms forming the summary shifts within AGT notions [66] as due to the incomplete understanding and verification of all AGT features [66]. The additional serious obstacle to direct comparison with the latter approach is that AGT operates with the so-called "center of gravity shift" (CGS) [66], which itself represents the integral characteristic for the total profile in comparison to the spectral distributed characteristic like asymmetry or shifts of individual Stark components considered here.

Regarding the existence of different electron and effective excitation levels population temperatures, it appears to be a reasonable assumption to some extent. Namely, in the stabilized arcs the forced water cooling and the special system of distributed gas inlets are causing the large radial gradients of plasma and gas parameters [2–4,7,9]. The heat and radiation transfers in such systems are very complicated thus leaving to some extent a space to support $T_a \neq T_e$ assumption. Anyway the question of the effective excitation levels population temperature could be resolved by experimental methods in the case of stabilized arcs and even in the case of non-stationary T-tube plasmas of [15,16]. It is useful to remind that analysis performed in [15] (where $T_a = T_e$ was assumed) had shown that the extent of influence of the Boltzmann and ω^4 factors on the asymmetry parameter, i.e. its sign and magnitude depends on the temperature, density and the value of unperturbed transition frequency. As a consequence, the character of $A(\Delta\lambda)$ behavior changes with respect to given line as well [15]. Also one should keep in mind that the correct inclusion of the Boltzmann and ω^4 factors into the asymmetry parameter calculations became possible only under the contour redefinition restraining the integration over negative detunings and the change of normalization. The consideration of the above factors involves, in fact, far more complicated and rich physics of plasma equilibrium than it was initially contemplated in [19] and later addressed in [31,32,36,39].

7 Conclusions

In corollary the results of the present work are formulated:

1. the theory of hydrogen spectral lines asymmetry in the parabolic basis of wave functions was further advanced with account of consistent treatment of QSE without perturbation expansion over quadrupole interaction in the contour and within impact approximation for description of electron broadening and quasistatic approximation for ion broadening;
2. as an example, the H_β profile asymmetry is studied through sensitivity of each individual Stark component to the following:
   (a) the constrained quadrupole interaction;
   (b) consistent consideration of quadratic Stark effect;
   (c) collision electron shifts;
   (d) the electron impact widths;
   (e) trivial asymmetry;
   (f) the profile redefinition with $\Delta\omega \geq -\omega_0$;
   (g) Boltzmann factor and multiplier, equal to the fourth power of cyclic frequency;
3. benchmark of theoretical results showed the potential for a rather well description of experimental data, based on fitting procedure that optimizes the values of
   (a) population temperature of excited levels that in principle differs from the one of electrons;
   (b) the electron impact widths values that are evidently overestimated due to the use of the diagonal approximation in the parabolic basis of wave functions;
   (c) the electron collision shifts values that control the location of the cross-over point in the asymmetry curve.

Thus the present complex study shows that the asymmetry of Stark contours of hydrogen lines in plasmas possesses the interesting manifold of dependences induced by numerous sources, which compete and interplay with each other in rather complex manner. That is why the initial perception that the asymmetry behavior could be explained entirely on the basis of quadrupole interaction (of ions with radiators) in quasistatic approximation [18, 20] or solely by the quadratic Stark effect [17,19] is unfounded.

The significant scaling and similarity of asymmetry versus the electron collision shifts and impact widths values, the quadrupole interaction and quadratic Stark effect shifts and the important dependence on the character of plasma equilibrium through the excited levels population temperature are established and studied. Hence it is

demonstrated that the asymmetry of hydrogen Stark profiles is the extremely sensitive function of the competing plasma broadening mechanisms and has undoubtedly fundamental significance.

It is shown that the consistent consideration of the Boltzmann factor and the dipole intensity scaling factor (equal to the fourth power of frequency) is possible only under the redefinition of the contour due to the constrained integration over the negative detunings.

In the new more rigorous approach of this work the result [14,15] of significant influence of quadratic Stark effect on intensities of Stark components and thus on profile asymmetry is confirmed. It seems necessary to perform the further study of asymmetry phenomena due to its fundamental significance for theoretical and experimental plasma spectroscopy with account of the dissolution effect of Stark components in the strong electric fields (see [27, 57]) and joint dynamical description of broadening by electrons and ions [46,51]. Confirmation of the role of the Boltzmann factor and the fourth power of frequency multiplier [48–50], plasma coupling [28,29,33–35], consistent account of contributions from octupole and the second order quadrupole interactions [20] are of no lesser importance. All this, however, exceeds the natural frames of the present work the volume of which is already large.

This work started during A.V.D.'s stay as a visiting professor at the University of Kiel in 2001, supported by DAAD. The work of A.V.D. was also partially supported by RRC "KI" grant for fundamental research N 20/2006-2007. The work of D.N. in 2001-2005 was supported by the University of Stockholm. The authors are very grateful to Prof. V. Helbig for providing the experimental data and to Dr. S. Sörge for the electron collision shifts values, generated within Green function approach and matching the experimental conditions. It is a pleasure to thank Dr. K. Grüntzmacher and Prof. V. Helbig for their interest and discussions encouraging this work. The cooperation and discussions with Prof. A.N. Starostin, Prof. S. Djurović, Prof. M.A. Gigosos and Prof. M.Á. González were very valuable for this study.

References

1. W. Filkenburg, Z. Phys. **70**, 375 (1931)
2. W.L. Wiese, D.R. Paquette, J.E. Solarski, Phys. Rev. **129**, 1225 (1963)
3. W.L. Wiese, D.E. Kelleher, D.R. Paquette, Phys. Rev. A **6**, 1132 (1972)
4. W.L. Wiese, D.E. Kelleher, V. Helbig, Phys. Rev. A **11**, 1854 (1975)
5. R.D. Bengtson, G.R. Chester, Phys. Rev. A **13**, 1762 (1976)
6. R.C. Preston, J. Phys. B **10**, 523, 1977
7. K. Grüntzmacher, W. Wende, Phys. Rev. A **18**, 2140 (1978)
8. D.E. Kelleher, N. Konjević, W.L. Wiese, Phys. Rev. A **20**, 1195, 1979.
9. V. Helbig, K.P. Nick, J. Phys. B **14**, 3573, 1981
10. F. Torres, M.A. Gigosos, S. Mar, J.Q.S.R.T. **31**, 265 (1984)
11. K.Grützmacher, B. Wende, in *Spectral Line Shapes*, edited by B. Wende (de Gruyter & Co., Berlin, N.Y, 1987), Vol. 4, p. 527
12. Z. Mijatović, M. Pavlov, S. Djurović, Phys. Rev. A **43**, 6095 (1991)
13. T. Boebel, Diploma thesis, Kiel University (1995)
14. A.V. Demura, V. Helbig, D. Nikolić, *Spectral Line Shapes* edited by C.A. Back, AIP Conference Proceedings 645, (N.Y., 2002), Vol. 12, pp. 318–324
15. S. Djurović, D. Nikolić, I. Savić, S. Sörge, A.V. Demura, Phys. Rev. E **71**, 036407 (2005)
16. A.V. Demura, S. Djurović, M.A. Gigosos, M.Á. González, M. Ćirišan, in *23rd SPIG* - Contributed papers, edited by L. Hadzievski, B. Marinković, N. Simonović (Institute of Physics, Belgrade, Serbia, 2006), p. 303
17. H.R. Griem, Z. Phys. **137**, 280 (1954)
18. L.P. Kudrin, G.V. Sholin, Doklady USSR **7**, 1015 (1963)
19. H.R. Griem, Phys. Rev. A **140**, 1140 (1965)
20. G.V. Sholin, Opt. Spectrosc. (USSR) **26**, 275 (1969); Preprint `IAE-1440`, I.V. Kurchatov institute of Atomic Energy, Moscow, 1967, p. 28 (*in Russian*)
21. E. Oks, G.V. Sholin, Opt. Spectrosc. (USSR) **33**, 217 (1972)
22. M.E. Bacon, J.Q.S.R.T. **13**, 1161 (1973); M.E. Bacon, J.Q.S.R.T. **17**, 501 (1977)
23. A.V. Demura, G.V. Sholin, J.Q.S.R.T. **15**, 881 (1975)
24. A.V. Demura, thesis, Kurchatov Insitute of Atomic Energy (1976), p. 176 (unpublished, *in Russian*)
25. A. de Kertanguy, N.T. Minh, N. Feautrier, J. Phys. B **12**, 365 (1979)
26. R.F. Joyce, L.A. Woltz, C.F. Hooper, Phys. Rev. A **35**, 2228 (1987)
27. B. d'Etat, J. Grumberg, E. Leboucher, H. Nguyen, A. Poquerusse, J. Phys. B **20**, 1733 (1987)
28. A.V. Demura, *Theory of Joint Distribution Functions of Microfield and its Spatial and Time Derivatives in Plasmas with Complex Ionization Composition*, Preprint `IAE-4632/6`, I.V. Kurchatov Institute of Atomic Energy, Moscow, 1988, p. 17 (*in Russian*)
29. A.V. Demura, First Moments of Unified Distribution Function of Electric Ion Microfield and it's Spatial and Time Derivatives in a Plasma with Weak Nonideality, in *Contributed Post-deadline Papers of ICSLS IXth*, 1988, edited by J. Szudy (Ossolineum, Wroclaw, Poland, 1989), pp. A39–A40
30. A.V. Demura, V.V. Pleshakov, G.V. Sholin, *Atlas of Detailed Stark Profiles in Dense Plasmas*, Preprint `IAE-5349/6`, I.V. Kurchatov Institute of Atomic Energy, Moscow, 1991, p. 97 (*in Russian*)
31. J. Halenka, Z. Phys. D **16**, 1 (1990)
32. A. Könies, S. Günter, J.Q.S.R.T. **52**, 825 (1994)
33. A.V. Demura, C. Stehlé, Effects of Microfield Nonuniformity in Dense Plasmas, in *Spectral Line Shapes*, edited by D. May, J. Drummond, E. Oks (AIP, New York, 1995), Vol. 8, pp. 177-208
34. A.V. Demura, D. Gilles, C. Stehlé, J.Q.S.R.T. **54**, 123 (1995)
35. A.V. Demura, JETP **83**, 60 (1996)
36. S. Günter, A. Könies, Phys. Rev. E **55**, 907 (1997)
37. C. Stehlé, D. Gilles, A.V. Demura, Eur. Phys. J. D **12**, 355 (2000)
38. A.V. Demura, D. Gilles, C. Stehlé, in *Spectral Line Shapes*, edited by J. Seidel, AIP Conf. Proc. **559** (AIP, N.Y., 2001), Vol. 11, p. 99107

39. S. Sörge, S. Günter, Eur. Phys. J. D **12**, 369 (2000)
40. A.V. Demura, unpublished (2000)
41. M.A. Gigosos, M.Á. González, unpublished (2001)
42. A.V. Demura, D. Nikolić, unpublished (2001)
43. A.V. Demura, G.V. Demchenko, *Spectral Line Shapes*, edited by E. Dalimier (Frontier Group, Paris, France, 2004), pp. 336–338.
44. A.V. Demura, G.V. Demchenko, D. Nikolić, *On Theory of Hydrogen Spectral Lines Asymmetry in Plasmas*, Preprint `IAE-6430/6` RRC "Kurchatov institute", Moscow, 2006, p. 37 (*in Russian*)
45. A.V. Demura, G.V. Demchenko, unpublished (2006)
46. M.A. Gigosos, M.Á. González, Study on the Asymmetry of the Balmer Lines, in *23rd SPIG* - Invited Lectures, Topical Invited Lectures, and Progress Reports, edited by. L. Hadzievski, B. Marinković, N. Simonović, AIP proceedings (AIP, N.Y., 2006), Vol. 876, pp. 294–300
47. H.R. Griem, Phys. Rev. A **27**, 2566 (1983); H.R. Griem, Phys. Rev. A **28**, 1596 (1983); H.R. Griem, Phys. Rev. A **38**, 2943 (1988)
48. I.I. Sobelman, *Introduction to the Theory of Atomic Spectra* (Pergamon Press, Oxford, 1972), p. 609
49. H.R. Griem, *Spectral Line Broadening by Plasmas* (Academic Press, N.Y., 1974); H.R. Griem, *Principles of Plasma Spectroscopy* (Cambridge University Press, 2005), p. 366
50. D.L. Huber, J.H. Van Vleck, Rev. Mod. Phys. **38**, 187 (1966)
51. M.A. Gigosos, M.Á. González, V. Cardeñoso, Spectrochim. Acta B **58**, 1489 (2003)
52. A.V. Demura, Statistical and Thermodynamical Aspects of Microfield Conception in Plasmas, in: *Encyclopedea of low temperature plasmas*, Series B, Reference additions, bases and banks of data, Thermodynamics of low temperature plasmas, edited by I.L. Iosilevsky, A.N. Starostin (Fizmatlit, M., 2004), Vol. III-1, pp. 163–202 (*in Russian*)
53. S. Chandrasekhar, Rev. Mod. Phys. **15**, 1 (1945)
54. L.D. Landau, E.M. Lifshits, *Nonrelativistic Quantum Mechanics* (GFML, Moscow, 1963) (*in Russian*)
55. N. Hoe, E. Banerjea, H.W. Drawin, L. Herman, J.Q.S.R.T. **5**, 835 (1965)
56. G.V. Sholin, A.V. Demura, V.S. Lisitsa, Sov. Phys. JETP **37**, 1057 (1973)
57. H.A. Bethe, E.E. Salpeter, *Quantum Mechanics of One- and Two- Electron Atoms* (Springer-Verlag, Heidelberg, 1957)
58. S. Sörge, private communication (2001)
59. L. Hitzschke, G. Röpke, T. Seifert, R. Zimmermann, J. Phys. B **19**, 2443 (1986)
60. G. Peach, Adv. Phys. **30**, 367 (1981)
61. P. Kepple, H.R. Griem, Phys. Rev. A **173**, 317 (1968)
62. S. Alexiou, A. Poquérusse, Phys. Rev. E **72**, 046404 (2005)
63. R. Stamm, D. Voslamber, J.Q.S.R.T. **22**, 1489 (1979)
64. R. Stamm, E. Smith, Phys. Rev. A **30**, 450 (1984)
65. R. Stamm, B. Talin, E.L. Pollock, C.A. Iglesias, Phys. Rev. A **34**, 4144 (1986)
66. E.A. Oks, *Stark Broadening of Hydrogen and Hydrogenlike Spectral Lines in Plasmas*, The Physical Insight (Alpha Science International Ltd., Oxford, U.K., 2006), p. 154
67. A. Escarguel, E. Oks, J. Richou, D. Volodko, Phys. Rev. E **62**, 2667 (2000)